Hydrogen-bonded donor–acceptor compounds for organic ferroelectric materials

Sachio Horiuchi,*[a] Reiji Kumai[a] and Yoshinori Tokura[abc]

Received (in Cambridge, UK) 7th December 2006, Accepted 17th January 2007
First published as an Advance Article on the web 12th February 2007
DOI: 10.1039/b617881b

Organic ferroelectrics are multifunctional candidates for future organic electronic and optical devices. In spite of their potential, only a few organic compounds are known to exhibit a ferroelectric transition. The conventional approach to ferroelectrics, in general, relies on the use of asymmetric dipolar molecules and/or substituents. Recently, distinct design strategies have been developed using the molecular compounds of binary- or multi-components, combined with ''non-covalent'' forces: charge-transfer interactions and/or hydrogen bonding. This article focuses on the supramolecular systems of hydrogen-bonded acid and base molecules. Ferroelectricity and a significant dielectric response, as well as an antiferroelectric ordering induced by proton transfer, are demonstrated in the hydrogen-bonded chains composed of 2,5-dihydroxy-*p*-benzoquinone derivatives and nitrogen-containing aromatic bases.

Introduction

Hydrogen (H)-bonded inorganic and organic compounds are often associated with various types of structural phase transitions including the transformation to a ferroelectric state. Ferroelectricity is a prominent phenomenon, constituting an important research field in condensed matter science, alongside conductivity, superconductivity, and magnetism.[1] In contrast to their fundamental scientific interest, ferroelectrics are currently of great interest in technological applications[1,2] from electronics to optics.

Ferroelectrics are polar (pyroelectric) crystals that exhibit spontaneous electric polarization, mostly belonging to the inorganic or organic–inorganic hybrid compounds such as barium titanate ($BaTiO_3$), sodium nitrite ($NaNO_2$), potassium dihydrogen phosphate (KH_2PO_4, KDP), and triglycine sulfate (TGS). The most important characteristic of ferroelectrics is that their spontaneous polarization can be reversed by inverting the external electric field. During polarization reversal for a coercive field, the electric displacement (D) as a function of the field (E) exhibits hysteresis (a D–E loop). In general, the ferroelectrics undergo a paraelectric-to-ferroelectric phase transition. The dielectric susceptibility usually obeys the Curie–Weiss law at high temperatures and exhibits a divergent-like increase to large values as the temperature approaches the phase transition point (Curie temperature T_c).

Sachio Horiuchi was born in Nara Prefecture, Japan in 1968. He received his PhD (1997) degree from Kyoto University under the supervision of Professor G. Saito. He was a research scientist at the Joint Research Center of Atom Technology (1997–2002). Since 2002, he has been a researcher at the Correlated Electron Research Center (CERC), National Institute of Advanced Industrial Science and Technology (AIST). He has worked on the development of new functional organic solids such as molecular conductors and dielectrics with novel phase transitions. His research is now focused on material design of new organic ferroelectrics.

Reiji Kumai was born in Aichi Prefecture, Japan in 1966. He obtained his PhD (1995) degree from the University of Tokyo under the supervision of Professor T. Sugawara. He was a research scientist at the Joint Research Center of Atom Technology (1995–2002) and a researcher at the National Institute of Advanced Interdisciplinary Research (1999–2001). In 2001, he joined the Correlated Electron Research Center (CERC), National Institute of Advanced Industrial Science and Technology (AIST) as a researcher, and is currently a senior researcher (2004–current). He has worked on the design and synthesis of novel organic solids such as molecular magnetic conductors. His research is now focused on the development of functional molecular systems and the precise structural analysis of correlated electron systems using synchrotron X-rays.

Yoshinori Tokura was born in Hyogo prefecture, Japan in 1954. He obtained his PhD (1981) degree from the University of Tokyo. He was an associate professor (1986–1993) and professor (1994–1995) at the Faculty of Science, University of Tokyo. Since 1995, he has been a professor at the Graduate School of Engineering, University of Tokyo, and since 2001 concurrently a Director of the Correlated Electron Research Center (CERC), National Institute of Advanced Industrial Science and Technology (AIST). He has worked on correlated electron science and technology with a focus on exploratory materials (high-temperature superconductors, Mott transition systems, organic semiconductors/ferroelectrics, orbitronic transition-metal oxides, multiferroics, etc.) and unconventional phenomena including photo-induced phase transitions.

---

[a] *Correlated Electron Research Center (CERC), National Institute of Advanced Industrial Science and Technology (AIST), Tsukuba, 305-8562, Japan. E-mail: s-horiuchi@aist.go.jp; Fax: +81-29-861-2586; Tel: +81-29-861-2945*
[b] *ERATO, JST, Tokura Multiferroics Project, c/o AIST, Tsukuba, 305-8562, Japan*
[c] *Department of Applied Physics, The University of Tokyo, Tokyo, 113-8656, Japan*

It is known that ferroelectric phase transitions are categorized as either an *order–disorder* or *displacive* type. In the former mechanism, orientational ordering of the asymmetric molecules or ions carrying permanent dipoles generates the spontaneous electric polarization. Sodium nitrite is a well-known example, in which the bent NO_2^- ion bears the electric dipole. In the *displacive* mechanism, the relative displacement between the different charges of the ions yields macroscopic polarization in the crystal. An example are the perovskite ferroelectrics, such as $BaTiO_3$.

The ferroelectric phenomenon and related properties can be utilized for a diverse range of technological applications.[1–3] The hysteresis behavior of the bistable polarization is directly applied to the non-volatile memory elements such as a ferroelectric random access memory (FeRAM) or a ferroelectric field-effect transistor (FeFET). The associated large dielectric susceptibility can be exploited for a high-capacity condenser and capacitor. These important electronic applications in thin film form are currently being investigated extensively using inorganic oxides.[3] The thermal change of spontaneous polarization (the pyroelectric effect), which is often large especially near the phase transition limit, is useful as a thermal detector. Furthermore, ferroelectric crystals exhibit unusually large electromechanical coupling, the coupling between the mechanical strain and electric polarization. The large electrostriction and piezoelectric effect are utilized in actuator, transducer, ultrasonic motors, piezoelectric elements, and *etc*. In addition, second-order optical non-linearity is observed as a second harmonic generation (SHG) activity and linear electro-optic effect. These properties may be applied to, for instance, frequency multipliers and light modulators.

If the above technologies could be fabricated using organic ferroelectrics, all-organic electronic and photonic devices, currently of great interest, could also be fabricated. It is increasingly important in organic electronics to establish design methods for materials, to control the properties of these materials to various external stimuli, such as electric, magnetic, mechanical, optical, thermal, and chemical. This article describes a new design strategy and prospective approaches to the fabrication of novel organic ferroelectrics.

General features of organic ferroelectric solids

Ferroelectricity is rarely encountered in low-molecular-weight organic compounds. Historically, the first report of a ferroelectric organic component (tartrate ion), the ferroelectric compound "Rochelle salt" [$KOOCCH(OH)CH(OH)COONa\cdot 4H_2O$], was in the 1920s.[4] Conventional organic ferroelectrics, in general, are of the order–disorder type, since the constituent molecules can be readily endowed with asymmetry. Other than with thiourea (**1**),[5] ferroelectricity is, in general, due to the orientational ordering of molecular dipoles in the single-component organic ferroelectrics as presented in Chart 1: 2,2,6,6-tetramethylpiperidine 1-oxyl (tanane) (**2**),[6] 1,6-bis(2,4-dinitrophenoxy)hexa-2,4-diyne (**3**),[7] trichloroacetamide (**4**),[8] and 1,1′-cyclohexane diacetic acid (**5**).[9] The dielectric constant is not large at room temperature (ε_{RT}, typically <10). Thiourea (T_c = 169 K) also has an asymmetric molecular structure, but the displacement of the molecular orientation is responsible for the displacive-type ferroelectricity with a larger ε_{RT} ($\sim$30) and significant spontaneous polarization ($\sim$3 μC cm^{-2}).[5] The best-known examples of organic ferroelectric solids are the ferroelectric polymers such as polyvinylidene fluoride[10] and copolymers of vinylidene fluoride with trifluoroethylene,[11] and these materials have been extensively studied.[12] The ferroelectricity of these polymers is based on the similar chemical origin of their polar side groups that carry the permanent dipoles. The ferroelectric polymers show very high spontaneous polarization ($\sim$10 μC cm^{-2}) and modest dielectric susceptibility ($\varepsilon < 100$). However, compared with other ferroelectric compounds, the coercive field for polarization reversal is extremely high, since its process requires the rotation of side groups around the main chain.

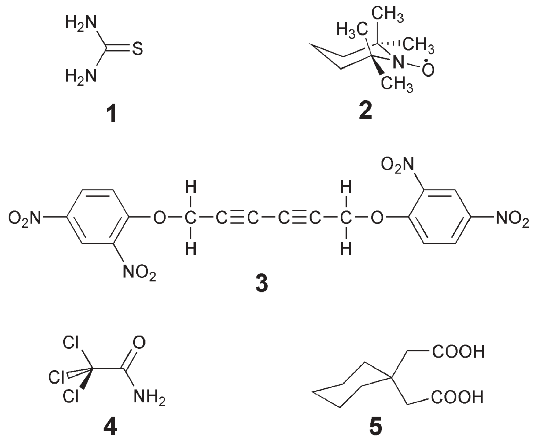

Chart 1 Single-component organic ferroelectrics of low molecular weight.

In contrast, molecular compounds of more than two different components may exhibit similar behavior to the $BaTiO_3$ compound, which undergoes a displacive ferroelectric transition when oppositely-charged ions are displaced. Until recently, this design strategy was applied only to the charge-transfer (CT) complexes composed of electron donor (**D**) and acceptor (**A**) molecules.[13] As exemplified by a complex of tetrathiafulvalene (TTF) and *p*-chloranil (QCl_4) (Fig. 1),[14] the molecules typically form π-stacked columns of alternating **D** and **A** (the "mixed stack") in one dimension. Occasionally the strong electron–lattice interaction (Peierls instability) triggers a molecular displacement, with **D**–**A** dimerization gaining the electric dipoles along the π-molecular stack as schematically illustrated in Fig. 1.[13,15,16] Alternatively, when the flat **D** or **A** molecules are flexible enough to bend, the spontaneous bending deformation can break symmetry, generating the polar **D**–**A** chains.[17] Such crystals can be either ferroelectric or antiferroelectric, depending on the three-dimensional arrangement of the polar chains. The ferroelectric and antiferroelectric ordering styles are shown in contrast by TTF–QCl_4[16] and its dimethyl-substituted analogue (DMTTF–QCl_4),[18] respectively. Apparently, these ferroelectric CT complexes do not require the asymmetric molecules to build the polar crystal. Their phase transition and dielectric properties have been closely controlled in various ways depending on chemical and physical modifications of the crystals. Among them, a quantum phase transition[18] and relaxor ferroelectricity,[19] both

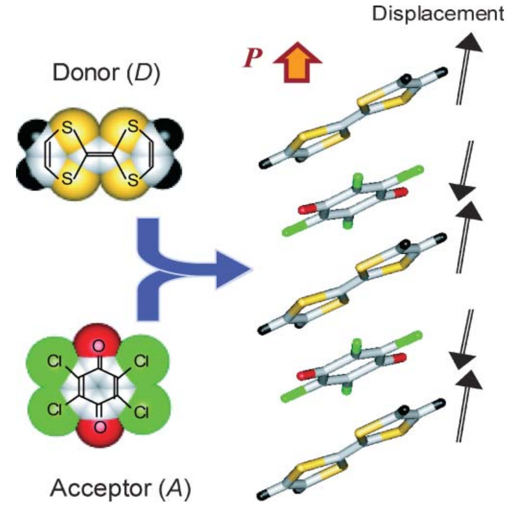

Fig. 1 Schematic representation of ferroelectric transition obtained from the displacement of the **D** and **A** molecules in charge-transfer complexes.

of which are currently attracting interest from both the academic and application perspectives, are realized in organic CT complexes. Recent reviews discuss the topics and chemical designs in detail.[20] One of the main properties of the CT complexes is the large dielectric constant, which varies from a few hundred up to *ca.* 2000. However, these CT complexes exhibit a relatively narrow charge gap and, hence, are bad insulators. The large dielectric loss tends to degrade spontaneous polarization, preventing various ferroelectric applications near room temperature. This drawback has been resolved by replacing the CT interaction with hydrogen bonding as shown below.

Hydrogen-bonded organic compounds as KDP analogues

Ferroelectricity and the related properties of hydrogen-bonded systems have been long studied in many inorganic salts.[1] The KH_2PO_4 (KDP) crystal is the best known ferroelectric.[21] The PO_4 ions are connected in a three-dimensional interpenetrating network of homonuclear O–H···O hydrogen bonds with a short O···O distance (2.50 Å). While the phase transition is triggered by the collective ordering of protons, the magnitude of spontaneous polarization arises mainly from the displacive motion of highly polarizable PO_4 ions. When the protons are replaced with deuterons, the Curie temperature T_c dramatically increases. Therefore, the roles of hydrogen bonding and proton dynamics are significant.[1,22–24] In particular, there have been numerous investigations of the mechanism of ferroelectricity. Blinc[23] proposed the proton tunneling model, which states that a different $H^+(D^+)$-tunneling frequency, due to the mass change, is responsible for the extremely large isotope effect on T_c in the KDP family. Recent progress in the experimental and theoretical details is described in ref. 24 and references cited therein.

The proton-transfer and dielectric properties of some hydrogen-bonded molecular crystals have been examined to explore organic analogues of ferroelectric KDP. Among the few known examples, 3,4-dihydroxy-3-cyclobutene-1,2-dione (squaric acid) has been the prototype,[25] in which the square planar $C_4O_4^{2-}$ ions are strongly hydrogen bonded with a short O···O distance (2.55 Å), forming a two-dimensional (2D) network of intermolecular O–H···O bonds (see Chart 2). In this crystal, the phase transition at $T = 373$ K is related to the collective order–disorder of the protons and exhibits a significant H/D isotope effect, in close analogy with KDP. Each squaric acid molecule preserves two protons in total during the proton transfer, similar to ice and KDP crystals. This constraint, called the "ice rule", characterizes the correlated motion of protons. It should be noted that the collective proton transfer is coupled with a geometric transformation of the π-conjugated system. For the proton-ordered low-temperature phase, the electric polarization occurs in the hydrogen-bonded molecular sheet. A large dielectric constant is observed parallel to this sheet. However, its temperature dependence is relatively weak and shows a rounded peak instead of the Curie–Weiss-type divergence typical of the ferroelectrics. This is because the antiferroelectric interlayer coupling cancels out the net polarization. True ferroelectric analogues of KDP are still to be disclosed in the purely organic system.

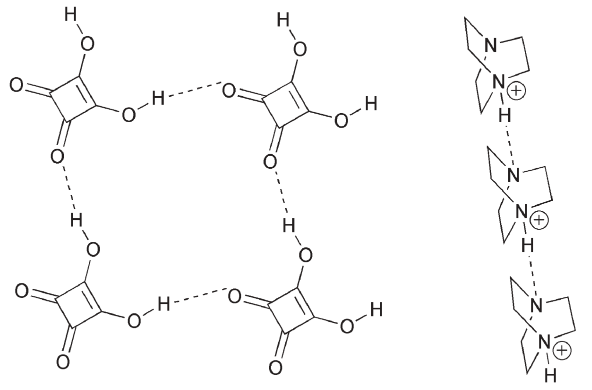

Chart 2 Intermolecular hydrogen bonding of the KDP-like ferro-/antiferroelectrics: squaric acid molecules (left) and mono-protonated diazabicyclo[2.2.2]octane ($Hdabco^+$) cations (right).

There are other interesting KDP-like dielectric crystals, derived from 9-hydroxyphenalenone (HPLN) molecules.[26] The hydrogen bonding is categorized to a zero-dimensional type, since it is confined within the HPLN molecule as a homonuclear O–H···O (O···O distance is 2.47 Å) bond between the hydroxy and carbonyl groups. As illustrated in Scheme 1, the electric dipole moment can be reversed by the intramolecular proton-transfer process and the simultaneous conversion of the π-conjugated forms, where this interconversion is a type of

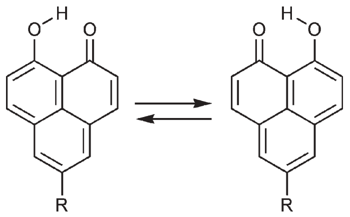

Scheme 1 Tautomerism of the 9-hydroxyphenalenones.

tautomerism.[27] Some of the HPLN derivatives exhibit a phase transition with proton ordering. The long-range order is an antiferroelectric type and accompanied by relatively small anomalies in the dielectric constant. These compounds show a rather low phase transition temperature (T_c), and even an incipient phase transition called "quantum paraelectricity" achieved in 5-bromo-HPLN (BrHPLN).[26b] The deuterium substitution gives rise to a significant effect on T_c. The deuteration induces the phase transition for BrHPLN. T_c is significantly increased for 5-methyl-HPLN. During the deuterium substitution, the O···O distance is fixed within the rigid HPLN molecule. The KDP family[28] and squaric acid,[25b] on the other hand, exhibit a significant elongation of the intermolecular O···O bond, known as the "Ubbelohde effect".[29] Therefore, the sizable isotopic effect on T_c in the HPLN family can be attributed solely to the different tunneling (quantum) motions between the proton and deuteron, without invoking the geometric effect. The analogous tautomerism has been studied in the *s-trans*-3-hydroxyenenones[30] and bisquaric acid,[31] which belong to the (quasi) one-dimensional hydrogen-bonded system. Besides the collective proton transfer, the system attracted considerable interest in terms of the possible dynamics of the protonic solitons, generated as the boundaries between the oppositely-polarized domains.[32]

Recently, Szafrański *et al.* reported some genuinely ferroelectric analogues of KDP using inorganic–organic binary compounds: the diazabicyclo[2.2.2]octane (dabco) salts with inorganic anions.[33] The mono-protonated amines ($Hdabco^+$ cations), which are not π- but σ-bonded molecules, form an infinite chain constructed of short homonuclear $N–H^+···N$ bonds (N···N distance: 2.84 Å, Chart 2). These salts displayed a well-defined electric hysteresis behavior with a very large spontaneous polarization (4–16 μC cm^{-2}). Also, T_c is near room temperature, being much higher than those of the KDP family. In the ReO_4 salt,[33a] the direction of the largest spontaneous polarization coincides with the hydrogen-bonded chain, proving that the reversal of polarity is due to the collective proton transfer processes along the chain.

Displacive-type ferroelectricity in neutral co-crystals

As a new strategy for developing organic ferroelectrics, our recent studies have simultaneously utilized both of the previously mentioned key features: the **DA**-type multi-component system and hydrogen bonding. This new methodology is simply supramolecular chemistry, as the proton-donor (acid) and -acceptor (base) molecules are combined with intermolecular hydrogen bonds. The hydrogen-bonded **DA**-type compounds are generally superior to the above CT complexes as insulators, advantageous in ferroelectricity and the corresponding applications.

The first discovered compounds[34] are neutral adducts consisting of phenazine (Phz) as the base (**A**) and 2,5-dihalo-3,6-dihydroxy-*p*-benzoquinones (chloranilic acid (H_2ca) and bromanilic acid (H_2ba)) as the acids (**D**). In the following discussion, the anilic acids[35] are designated as H_2xa. It should be noted that both the acid and base are π-conjugated molecules.

Before discussing their electric properties in detail, we will note some important characteristics of the component H_2xa molecules. First, the molecules have an excellent ability to form various **DA**-type compounds because they can adopt various degrees of protonation and oxidation as illustrated in Scheme 2. They usually serve as strong dibasic acids (pK_1 = 0.73, pK_2 = 3.08 for H_2ca)[36] in combination with various bases. Neutral adducts or proton-transferred monovalent or divalent salts are formed depending on the basicity and/or **D**–**A** molar ratio.[37,38] They also work as strong electron acceptors. Therefore, many CT salts have been prepared with various electron donors, such as TTF derivatives[39] and decamethylferrocene.[40] Most of these salts include simple deprotonated Hxa^- or divalent xa^{2-} species instead of the reduced forms. The **D** molecules are oxidized but do not accept protons from these acids. The CT salt with TTF[41] includes the reduced form, two-electrons–two-protons-accepted H_4ca (tetrahydroxy-*p*-dichlorobenzene), in addition to the deprotonated ca^{2-} dianion, as formulated by $(TTF^+)_2(ca^{2-})(H_4ca)$. Accordingly, the reduction of H_2xa with strong donors in solution should be accompanied by such a proton disproportionation. The other novel feature is the molecular topology that exhibits a π-conjugated fragment of the β-diketone enol (enolone, HO–C=C–C=O) as given by the chemical formula in Scheme 2. This conjugated form is known to yield strong intra- or intermolecular interactions, called "resonance-assisted hydrogen bonding (RAHB)".[42] There are two enolone fragments linked with each other with a short O···O distance within the molecules. These oxygen atoms can connect tightly with the base molecules through bifurcated O···H···N bonding, which may vary from a neutral to ionic form (Chart 3). Furthermore, the H_2xa and deprotonated Hxa^- and xa^{2-} molecules are found to form various hydrogen bonds with themselves or the solvent molecules, constructing a variety of supramolecular synthons.

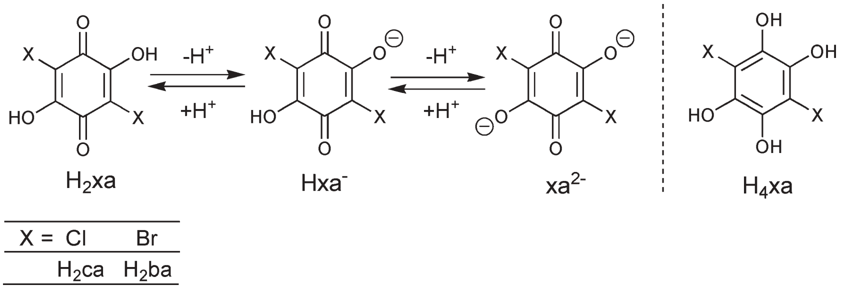

Scheme 2 The 2,5-dihydroxy-*p*-benzoquinone derivatives (H_2xa) and the corresponding proton-transfer processes. The molecule on the right is the two-electrons–two-protons-accepted species observed in the CT salt with TTF.

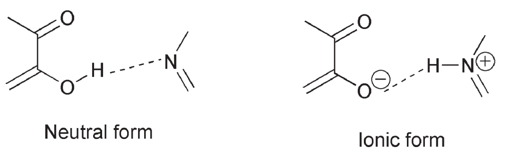

Chart 3 Hydrogen bonding types between the H_2xa and base molecules.

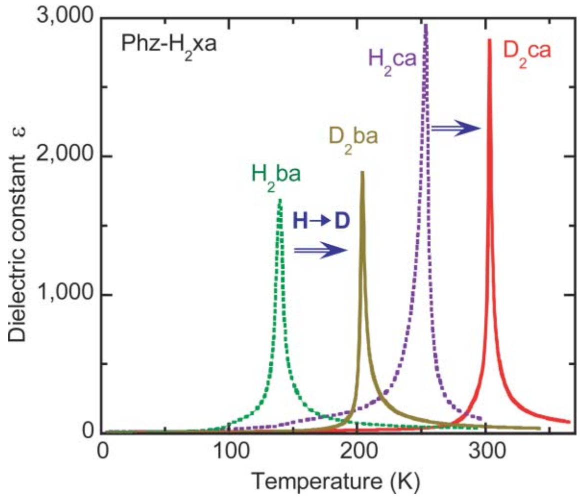

Fig. 2 A plot of the dielectric constant as a function of temperature, of Phz–H_2xa and the corresponding deuterated co-crystals.[34]

The ferroelectric Phz–H_2xa co-crystals reveal a very large dielectric constant (ε), exceeding 100 even at room temperature (Fig. 2), and obey the Curie–Weiss law, $\varepsilon = C/(T - \theta)$, increasing divergently up to 2000–3000 at the Curie temperature (T_c = 253 and 138 K for **D** = H_2ca and H_2ba, respectively).[34] The observed ε values are the largest among the organic ferroelectrics. The T_c significantly increases with an applied pressure or through deuteration of the H bonds, and reaches room temperature with an applied pressure of 0.60 GPa or through the deuterium substitution of the Phz–H_2ca crystal.

Fig. 3 shows the polarization hysteresis curves for Phz–H_2ca and its deuterated crystals.[34] The electric polarization is nearly linear with the applied electric field in the high-temperature phase, being typical of the paraelectric state. For temperatures below T_c, the clear polarization hysteresis curve validates the ferroelectricity. The Phz–D_2ca crystal exhibits room-temperature ferroelectricity as indicated in Fig. 3b. Spontaneous polarization in the Phz–H_2xa crystals and their deuterated analogs is as large as 0.7–0.8 μC cm^{-2} at low temperatures. The displacive-type mechanism was suggested from magnitude of the polarization. Saito *et al.* confirmed this from the heat capacity measurements, demonstrating small entropy changes at T_c compared with that expected for the configurational order–disorder mechanism.[43]

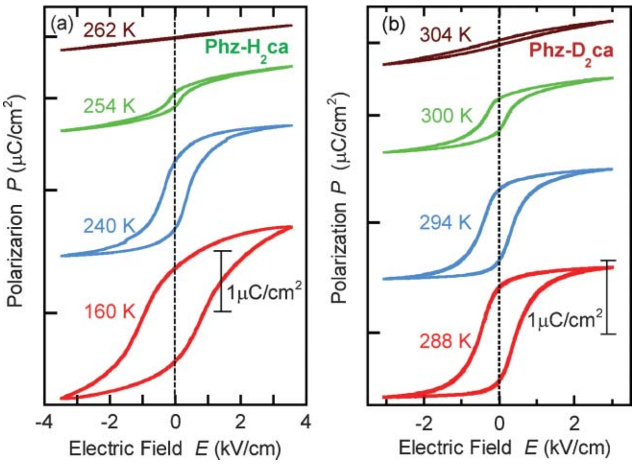

Fig. 3 Hysteresis loops of electric polarization at various temperatures for (a) Phz–H_2ca and (b) Phz–D_2ca crystals, as direct evidence of ferroelectricity.[34]

The structures of the Phz–H_2xa co-crystals (Fig. 4) belong to the monoclinic system. In the paraelectric structure with the nonpolar space group $P2_1/n$, both molecules are symmetric on the center of inversion and electrically neutral since the two protons are not transferred to the base molecules. The **D** and **A** molecules form the respective π-stacked columns along the *b* direction. It is important to note that the **D** and **A** molecules are connected with each other by a heteronuclear O–H···N bond through a short O···N distance (2.72 Å). This intermolecular hydrogen bonding is an infinite supramolecular chain of alternating **D** and **A** molecules. With the loss of the *n*-glide crystal symmetry due to the phase transition, the low-temperature structure belongs to the polar space group $P2_1$, yielding a polarity along the crystallographic *b* axis. The phase

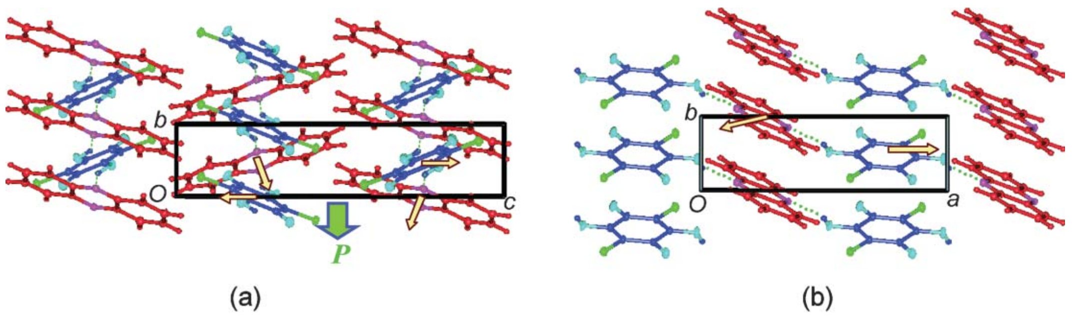

Fig. 4 Molecular arrangement in the ferroelectric phase of Phz–H_2ca co-crystal from single crystal X-ray diffraction measurements at 160 K.[34a] (a) The crystal structure with macroscopic electric polarization *P* viewed along the crystallographic *a* axis. (b) The arrangement of molecules on the $z = 3/4$ plane. The dotted lines and orange arrows indicate hydrogen bonds and the directions of molecular displacement from the paraelectric symmetric structure, respectively.

transition barely modifies the molecular structures and, hence, the molecules remain neutral in both phases. The symmetry is broken because of a molecular displacement as illustrated by arrows in Fig. 4.

The O–H···N bonding exhibiting the significant H/D isotope effect is an important part of the ferroelectricity. However, the present system appears to be distinct from KDP and its analogous compounds. First, all these hydrogen bonds preserve the asymmetric O–H···N form even in the low-temperature ferroelectric structures. Therefore, the site-to-site proton transfer process cannot be the origin of the polarization reversal. The other distinct features appear in the change of the hydrogen-bonding geometry. The H/D substitution increases T_c and the O···N distance, in agreement with the general behavior of the KDP family. However, the substitution of Cl for Br in the H_2xa results in an opposite behavior. The T_c increases in spite of the shortened O···N distance. The application of hydrostatic pressure also raises the T_c, in contrast to the KDP. Therefore, the observed T_c change cannot be correlated with the geometric effect. From these observations, the Phz–H_2xa system should be distinguished from the KDP-type ferroelectrics.

The observed large spontaneous polarization and large dielectric response in the Phz–H_2xa co-crystals is unexpected, because all the constituent molecules remain nearly nonpolar and electrically neutral even in the ferroelectric phase. The calculated dipole in the crystal, as a simple sum of the molecular dipoles and the contributions from a displacement, cannot account for the observed large polarization.[34] In the field of ferroelectrics, the origin and evaluation of the electric polarization is a critical issue. The exact evaluation of electric polarization, especially for the infinite lattice system with covalent bonding character, was established only a decade ago using the modern theory based on the Berry-phase picture.[44] The fascinating feature demonstrated is that the polarization can be amplified (by a factor of ≈ 3) through the electron transfer interaction, shown for many displacive-type ferroelectrics[45] having covalent bonds. This new theoretical approach, using the state-of-art first-principle calculations,[34,46] has reproduced the large polarization on the Phz–H_2ca, suggesting that the covalent nature of bonds plays an important role in the crystal. The covalency in the molecular crystals should correspond to a significant charge density on the intermolecular space, the actual case for the intermolecular O–H···N bonds for the present crystals. The partially covalent character in the hydrogen bonds has been argued in other dielectrics[46] and even in ice.[47] In terms of the displacement along with the partially covalent bonds, the Phz–H_2xa co-crystals could be viewed as a molecular-crystal version of "$BaTiO_3$".

Toward KDP-type ferroelectrics from proton donor–acceptor compounds

When the different molecules are joined as binary- or multi-component compounds, their intermolecular hydrogen bonds should acquire more or less an asymmetric potential for moving protons. This is typically the case for the heteronuclear type as exemplified by the O–H···N bond in the above Phz–H_2xa co-crystals. One may thus imagine that the proton transfer in such compounds should be a limited case, compared with the symmetric homonuclear type like the above KDP analogues. Nevertheless, Reetz *et al.* have postulated an intermolecular proton transfer in the heteronuclear hydrogen bonds responsible for thermally-induced phase transition and thermochromism in the co-crystal of 4,4′-bipyridine with squaric acid,[48] formed by short hydrogen bonds (N···O distance 2.60–2.61 Å). Moreover, recent neutron diffraction studies on some strongly hydrogen-bonded **DA**-type compounds have actually visualized novel, thermally-induced proton migration; co-crystals of 4-methylpyridine with pentachlorophenol,[49] of 4,4′-bipyridine with pyromellitic acid,[50] and of urea with phosphoric acid.[51] These bases and acids are appropriately selected with a similar proton affinity to guarantee that the protons of the heteronuclear hydrogen bonds can easily attach to both molecules. Such a proton delocalization between the base and acid can strengthen the covalent-bonding character of the hydrogen bonds.[52] Since analogous proton dynamics are required for the KDP-type ferroelectricity, these observations have convinced us that supramolecules are also well suited for this purpose.

Indeed, an antiferroelectric phase transition accompanying the collective proton ordering has recently been found in a proton-transferred monovalent salt of H_2ca with 5,5′-dimethyl-2,2′-bipyridine (55DMBP) (Scheme 3).[53] The dielectric susceptibility is large (≈ 140) and shows a rounded peak indicative of an antiferroelectric phase transition near room

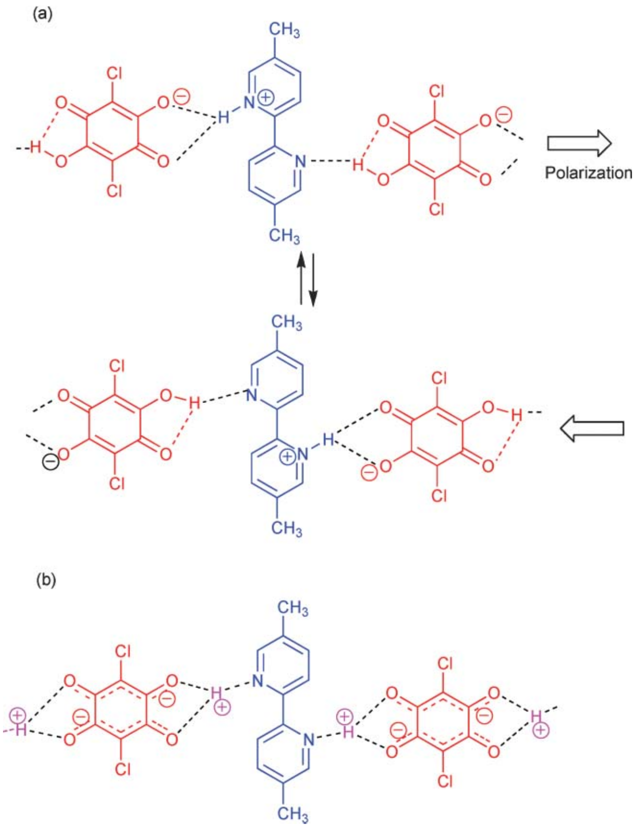

Scheme 3 Hydrogen-bonding structures of [H–55DMBP][Hca] in (a) the low-temperature (ordered) and (b) high-temperature (disordered) phases.

temperature (T_c = 318 K) (Fig. 5). The temperature dependence is similar to that observed for the antiferroelectric squaric acid[25b] but is distinct from the divergent behavior typical of the ferroelectrics obeying the Curie–Weiss law. The substitution of the protons with deuterons significantly raises the T_c, typical of the KDP analogues. The dielectric properties are highly anisotropic with a large response only along the hydrogen-bonded chain. These observations highlight the important role of hydrogen bonding on the phase transition. The powdered sample also exhibits a discernible thermochromism as a color change varying from violet to reddish brown upon heating above T_c. This is evident in the slight decrease of the intensity of the 2.4 eV band in the optical absorption spectra as indicated in the inset of Fig. 5. This thermochromic band is assigned to the absorption of the Hca^- monoanions. Its intensity change, as well as the dielectric response, is related to the proton transfer dynamics discussed below.

The crystal structure (Fig. 6)[53] at 100 K belongs to the triclinic system (space group: $P\bar{1}$). The monovalent $H\text{–}55DMBP^+$ cation in the planar *trans* form and the Hca^- anions are alternately linked, forming an infinite linear chain with intermolecular hydrogen bonding. This structure stands for the low-temperature (LT) phase. All the protons appear to be in a long-range order. The O–H and $N\text{–}H^+$ bonds are all aligned in the same direction. The alternating O–H···N and $N\text{–}H^+\cdots O^-$ constitute a polar chain, as illustrated in Scheme 3a. In this case, the polarization could be reversed between the two degenerate states, related by transferring all the protons simultaneously. In the actual crystal, the existence of a neighboring chain with an opposite polarity cancels out the net polarization; the molecular arrangement parallel to the *ab* plane constitutes a polar layer but the corresponding interlayer coupling is antiferroelectric due to inversion symmetry. This agrees with the antiferroelectric character of the dielectric response.

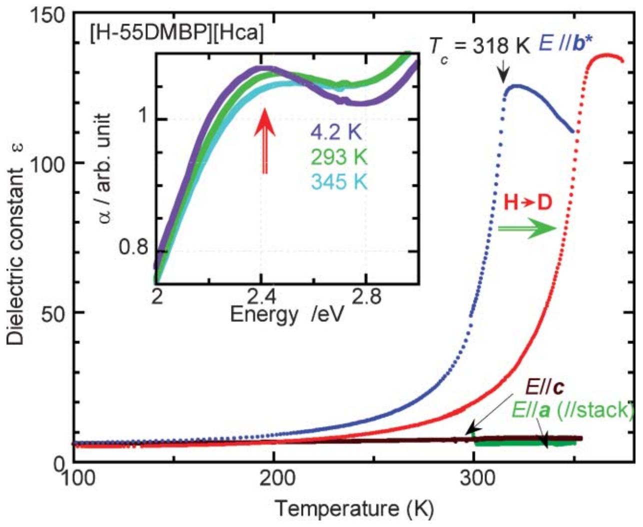

Fig. 5 A plot of the dielectric constant as a function of temperature of [H–55DMBP][Hca] and the 76%-deuterated crystals.[53] The ac field (100 kHz) was applied parallel to the *a*, *b**, and *c*-axis of the [H–55DMBP][Hca] crystal. The inset is the thermal change of the electronic optical absorption spectra of [H–55DMBP][Hca] measured on a KBr pellet.

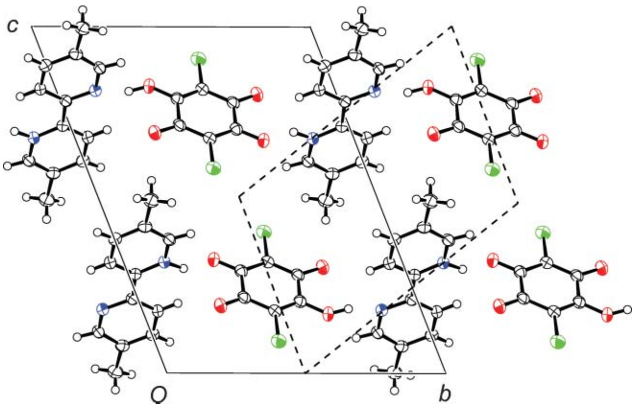

Fig. 6 Crystal structure of the [H–55DMBP][Hca] at 100 K (low-temperature phase).[53] The dotted square highlights the corresponding unit cell of the high-temperature phase.

In contrast, the crystal structure of the high-temperature (HT) phase (triclinic, space group: $P\bar{1}$) exhibits disorder. First, the unit cell volume is reduced in half from the LT form indicated by a dotted square in Fig. 6. All the molecules are located on the centers of inversion. Hence, the corresponding hydrogen bonds do not result in polar chains. The electron distribution on the hydrogen bond for both phases has been analyzed using the maximum entropy method (MEM), recently developed with the use of high-resolution diffraction data of synchrotron X-ray measurements.[54] In the LT form, electron density distributions in the O–H···N (Fig. 7a) and $N\text{–}H^+\cdots O^-$ regions (Fig. 7b) appear as electron clouds of

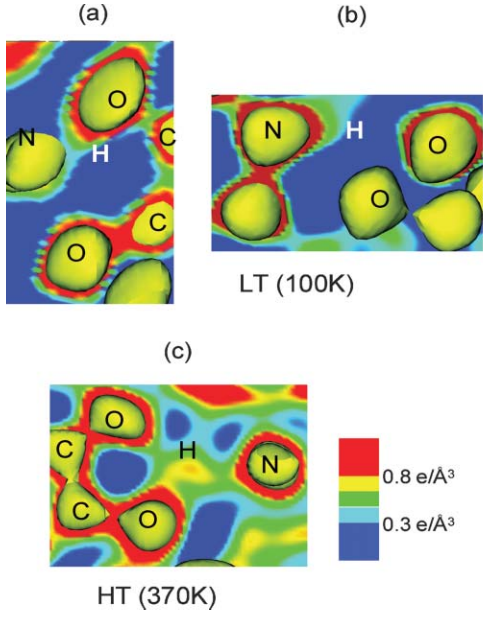

Fig. 7 The 3D electron density of (a) the neutral O–H···N and (b) ionic $N\text{–}H^+\cdots O^-$ hydrogen bonds in the LT phase (T = 100 K) and (c) corresponding region at the HT phase (T = 370 K) obtained from the maximum entropy method (MEM) analysis as an equal-density contour surface with contour map projecting on the plane containing the hydrogen-bonding site.[53] The equicontour level in the 3D maps is 1.5 e Å^{-3} and the contour maps are drawn from 0.3 e Å^{-3} (blue) to 0.8 e Å^{-3} (red).

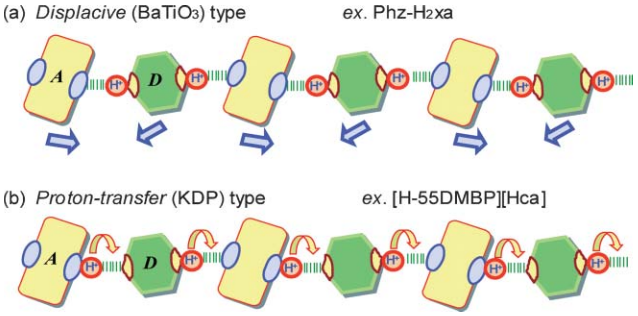

Fig. 8 Schematic diagram of the construction of polar structures on the hydrogen-bonded 1D chains of the proton donor (**D**) and acceptor (**A**) molecules. (a) Displacive-type ferroelectricity with the molecular displacement (thick arrows). (b) KDP-type ferroelectricity with proton dynamics. Rounded arrows indicate collective proton transfer during the polarization reversal.

distorted OH and NH ellipses, respectively, indicating the localized electrons of the hydrogen atoms. The electron density, however, for the HT form is extensively delocalized, with the maximum around the averaged (centered) position (Fig. 7c). The O···H···N hydrogen bond may be viewed as a four-center–five-electron covalent bond (Scheme 3b). This picture differs from the proton dynamics in a simple double-wells potential, which should result in double maxima in the electron density of a hydrogen atom. Such disorder also precludes the neutral or divalent form for the HT phase and, hence, the molecules should be at the intermediate state, *i.e.* the monovalent form. Considering the nature of the phase transition as described above, the collective proton transfer illustrated in Scheme 3a should be a plausible mechanism of polarity reversal. This is exactly what was first expected to achieve the KDP-type ferroelectricity.

The schematic drawings in Fig. 8 show the displacive-type and KDP-type ferroelectricity in similar supramolecular chains in contrast. These design strategies should not be limited to the compounds of proton **D** and **A** molecules. For example, a similar approach to ferroelectrics may be applied to more complicated systems that serve simultaneously as the proton **DA** and electron **DA** type and may undertake a cooperative proton–electron transfer (PET).[55] Let us consider the case of the quinhydron crystal as a typical example.[56] In this crystal, the proton-donating electron donor, hydroquinone, and the proton-accepting electron acceptor, *p*-benzoquinone, form the mixed π-molecular stack with CT interactions, alternately linked with O–H···O hydrogen bonds. If such a molecular crystal were to experience molecular displacement, or collective PET, the nonpolar structure made from these symmetric molecules could possibly turn to the similar polar form.

Conclusions

In this article, we have demonstrated that hydrogen bonding between proton donor and acceptor molecules is a way to produce novel organic ferroelectrics. The first discovered Phz–H_2xa co-crystals are similar to the displacive-type ferroelectrics. Furthermore, the proton dynamics with a large dielectric response in the H–55DMBP salt convinces us that this approach is also a potential route to genuine organic analogues of the KDP-type ferroelectrics. These would be good examples of the close association between supramolecular chemistry and organic electronics.

Ferroelectricity in organic solids is quite important for the production of all-organic electronic and photonic devices. Hence, supramolecular chemistry will be useful for this purpose. As an example of an application, several investigations of ferroelectric FET (FeFET) have recently utilized ferroelectric polymers to fabricate "entirely organic" permanent memory devises.[57] Organic semiconductors exhibiting good performance properties can be progressively applied to the active layer. Compared with ferroelectric polymers having a very high coercive field (E_c), the E_c of the Phz–H_2xa co-crystals is 2–3 orders of magnitude lower. Similar **DA** molecular compounds could be useful devices that operate at much lower voltages. Moreover, the ferroelectric co-crystals exhibit a large permittivity (κ) exceeding 100, promising for high-κ elements including capacitors. The [H–55DMBP][Hca], as well as the squaric acid, salts exhibit a large κ ($>$100) above the phase transition temperature. The high-κ applications often require the permittivity to be constant over a wide temperature range. The collective proton dynamics in the latter compounds, though not exhibiting a ferroelectric ordering, would satisfy this requirement since the permittivity exhibits a modest temperature dependence compared with the strong T-dependence in the ferroelectrics. Proton dynamics has attracted interest for potential diverse applications, from electronics to optics, as well as in the fundamental role in many chemical reactions and biological functions.[58] Ferroelectricity should be a challenging target as one of the highlighting functions. Therefore, further exploratory studies on a variety of ferroelectric and related materials, using low-molecular-weight organic systems, should be of increasing importance in the development of new functionality in an emergent research field.

Acknowledgements

The authors would like to thank F. Ishii, Y. Okimoto, and N. Nagaosa for collaborations on many subjects, and T. Hasegawa and H. Sawa for useful discussions and helpful advice with the experiments. This study was partly supported by a Grant-in-Aid for Scientific Research (No. 18750133) by the Ministry of Education, Culture, Sports, Science and Technology of Japan.

References

1 M. E. Lines and A. M. Glass, *Principles and Applications of Ferroelectrics and Related Materials*, Oxford University Press, New York, 1977.
2 K. Uchino, *Ferroelectric Devices*, Marcel Dekker, New York, 2000.
3 M. Dawber, K. M. Rabe and J. F. Scott, *Rev. Mod. Phys.*, 2005, **77**, 1083–1130.
4 J. Valasek, *Phys. Rev.*, 1921, **17**, 475–481.
5 G. J. Goldsmith and J. G. White, *J. Chem. Phys.*, 1959, **31**, 1175–1187.
6 D. Bordeaux, J. Bornarel, A. Capiomont, J. Lajzerowicz-Bonneteau, J. Lajzerowicz and J. F. Legrand, *Phys. Rev. Lett.*, 1973, **31**, 314–317.
7 G. F. Lipscomb, A. F. Garito and T. S. Wei, *Ferroelectrics*, 1980, **23**, 161–172.

8 Y. Kamishima, Y. Akishige and M. Hashimoto, *J. Phys. Soc. Jpn.*, 1991, **60**, 2147–2150.

9 J. Kroupa, P. Vanek, R. Krupkova and Z. Zikmund, *Ferroelectrics*, 1997, **202**, 229–234.

10 T. Furukawa, M. Date and E. Fukada, *J. Appl. Phys.*, 1980, **51**, 1135–1141.

11 T. Yagi, M. Tatemoto and J. Sako, *Polym. J. (Tokyo)*, 1980, **12**, 209–223.

12 T. Furukawa, *Phase Transitions*, 1989, **18**, 143–211.

13 Y. Tokura, S. Koshihara, Y. Iwasa, H. Okamoto, T. Komatsu, T. Koda, N. Iwasawa and G. Saito, *Phys. Rev. Lett.*, 1989, **63**, 2405–2408.

14 J. B. Torrance, A. Girlando, J. J. Mayerle, J. I. Crowley, V. Y. Lee and B. Batail, *Phys. Rev. Lett.*, 1981, **47**, 1747–1750.

15 H. Okamoto, T. Mitani, Y. Tokura, S. Koshihara, T. Komatsu, Y. Iwasa, T. Koda and G. Saito, *Phys. Rev. B: Condens. Matter*, 1991, **43**, 8224–8232.

16 M. Le Cointe, M. H. Lemée-Cailleau, H. Cailleau, B. Toudic, L. Toupet, G. Heger, F. Moussa, P. Schweiss, K. H. Kraft and N. Karl, *Phys. Rev. B: Condens. Matter*, 1995, **51**, 3374–3386.

17 S. Horiuchi, R. Kumai, Y. Okimoto and Y. Tokura, *J. Am. Chem. Soc.*, 1999, **121**, 6757–6758.

18 S. Horiuchi, Y. Okimoto, R. Kumai and Y. Tokura, *Science*, 2003, **299**, 229–232.

19 S. Horiuchi, R. Kumai, Y. Okimoto and Y. Tokura, *Phys. Rev. Lett.*, 2000, **85**, 5210–5213.

20 (*a*) S. Horiuchi, R. Kumai, Y. Okimoto and Y. Tokura, *Chem. Phys.*, 2006, **325**, 78–91; (*b*) S. Horiuchi, T. Hasegawa and Y. Tokura, *J. Phys. Soc. Jpn.*, 2006, **75**, 051016.

21 G. Busch and P. Scherrer, *Naturwissenschaften*, 1935, **23**, 737.

22 J. C. Slater, *J. Chem. Phys.*, 1941, **9**, 16–33.

23 R. Blinc, *J. Phys. Chem. Solids*, 1960, **13**, 204–211.

24 S. Koval, J. Kohanoff, J. Lasave, G. Colizzi and R. L. Migoni, *Phys. Rev. B: Condens. Matter*, 2005, **71**, 184102.

25 (*a*) E. J. Samuelsen and D. Semmingsen, *J. Phys. Chem. Solids*, 1977, **38**, 1275–1283; (*b*) G. A. Samara and D. Semmingsen, *J. Chem. Phys.*, 1979, **71**, 1401–1407; (*c*) Y. Moritomo, Y. Tokura, H. Takahashi and N. Mori, *Phys. Rev. Lett.*, 1991, **67**, 2041–2044; (*d*) N. Dalal, A. Klymachyov and A. Bussmann-Holder, *Phys. Rev. Lett.*, 2006, **81**, 5924–5927.

26 (*a*) T. Sugawara, T. Mochida, A. Miyazaki, A. Izuoka, N. Sato, Y. Sugawara, K. Deguchi, T. Moritomo and Y. Tokura, *Solid State Commun.*, 1992, **83**, 665–668; (*b*) T. Mochida, A. Izuoka, T. Sugawara, Y. Moritomo and Y. Tokura, *J. Chem. Phys.*, 1994, **101**, 7971–7973; (*c*) R. Kiyanagi, A. Kojima, H. Kimura, M. Watanabe, Y. Noda, T. Mochida and T. Sugawara, *J. Phys. Soc. Jpn.*, 2005, **74**, 613–620.

27 T. Sugawara and I. Takasu, *Adv. Phys. Org. Chem.*, 1999, **32**, 219–265.

28 (*a*) M. Ichikawa, K. Motida and N. Yamada, *Phys. Rev. B: Condens. Matter*, 1987, **36**, 874–876; (*b*) M. I. McMahon, R. J. Nelmes, W. F. Kuhs, R. Dorwarth, R. O. Piltz and Z. Tun, *Nature*, 1990, **348**, 317–319.

29 A. R. Ubbelohde and K. J. Gallagher, *Acta Crystallogr.*, 1955, **8**, 71–83.

30 Y. Moritomo, Y. Tokura, T. Oohashi, T. Kojima and A. Itsubo, *J. Chem. Phys.*, 1992, **96**, 8507–8513.

31 I. Takasu, T. Sugawara and T. Mochida, *J. Phys. Chem. B*, 2004, **108**, 18495–18499.

32 Y. Kashimori, T. Kikuchi and K. Nishimoto, *J. Chem. Phys.*, 1982, **77**, 1904–1907.

33 (*a*) M. Szafrański, A. Katrusiak and G. J. McIntyre, *Phys. Rev. Lett.*, 2002, **89**, 215507; (*b*) A. Katrusiak and M. Szafrański, *Phys. Rev. Lett.*, 1999, **82**, 576–579.

34 (*a*) S. Horiuchi, F. Ishii, R. Kumai, Y. Okimoto, H. Tachibana, N. Nagaosa and Y. Tokura, *Nat. Mater.*, 2005, **4**, 163–166; (*b*) S. Horiuchi, R. Kumai and Y. Tokura, *J. Am. Chem. Soc.*, 2005, **127**, 5010–5011.

35 S. Kitagawa and S. Kawata, *Coord. Chem. Rev.*, 2002, **224**, 11–34.

36 K. Wallenfels and K. Friedrich, *Chem. Ber.*, 1960, **93**, 3070–3082.

37 (*a*) M. B. Zaman, M. Tomura and Y. Yamashita, *Chem. Commun.*, 1999, 999–1000; (*b*) M. B. Zaman, M. Tomura and Y. Yamashita, *Org. Lett.*, 2000, **2**, 273–275; (*c*) M. B. Zaman, M. Tomura and Y. Yamashita, *J. Org. Chem.*, 2001, **66**, 5987–5995; (*d*) M. B. Zaman, K. A. Konstantin and J. A. Ripmeester, *Cryst. Growth Des.*, 2004, **4**, 585–589.

38 (*a*) H. Ishida and S. Kashino, *Acta Crystallogr., Sect. C: Cryst. Struct. Commun.*, 1999, **C55**, 1149–1152; (*b*) H. Ishida and S. Kashino, *Acta Crystallogr., Sect. C: Cryst. Struct. Commun.*, 1999, **C55**, 1923–1926.

39 (*a*) S. Horiuchi, H. Yamochi, G. Saito, K. Sakaguchi and M. Kusunoki, *J. Am. Chem. Soc.*, 1996, **118**, 8604–8622; (*b*) S. Horiuchi, H. Yamochi, G. Saito and K. Matsumoto, *Synth. Met.*, 1997, **86**, 1809–1810; (*c*) M. B. Zaman, Y. Morita, J. Toyoda, H. Yamochi, G. Saito, N. Yoneyama, T. Enoki and K. Nakasuji, *Chem. Lett.*, 1997, 729–730; (*d*) M. B. Zaman, J. Toyoda, Y. Morita, S. Nakamura, H. Yamochi, G. Saito, K. Nishimura, N. Yoneyama, T. Enoki and K. Nakasuji, *J. Mater. Chem.*, 2001, **11**, 2211–2215; (*e*) Y. Morita, S. Maki, M. Ohmoto, H. Kitagawa, T. Okubo, T. Mitani and K. Nakasuji, *Org. Lett.*, 2002, **4**, 2185–2188.

40 M. B. Zaman, M. Tomura and Y. Yamashita, *Inorg. Chim. Acta*, 2001, **318**, 127–134.

41 M. K. Kabir, H. Tobita, H. Matsuo, K. Nagayoshi, K. Yamada, A. Adachi, Y. Sugiyama, S. Kitagawa and S. Kawata, *Cryst. Growth Des.*, 2005, **3**, 791–798.

42 G. Gilli, F. Bellucci, V. Ferretti and V. Bertolasi, *J. Am. Chem. Soc.*, 1989, **111**, 1023–1028.

43 K. Saito, M. Amano, Y. Yamamura, T. Tojo and T. Atake, *J. Phys. Soc. Jpn.*, 2006, **75**, 033601.

44 (*a*) R. D. King-Smith and D. Vanderbilt, *Phys. Rev. B: Condens. Matter*, 1993, **47**, 1651–1654; (*b*) R. Resta, *Rev. Mod. Phys.*, 1994, **66**, 899–915.

45 R. E. Cohen, *Nature*, 1992, **358**, 136–138.

46 F. Ishii, N. Nagaosa, Y. Tokura and K. Terakura, *Phys. Rev. B: Condens. Matter*, 2006, **73**, 212105.

47 T. W. Martin and Z. S. Derewenda, *Nat. Struct. Biol.*, 1999, **6**, 403–407.

48 M. T. Reetz, S. Höger and K. Harms, *Angew. Chem., Int. Ed. Engl.*, 1994, **33**, 181–183.

49 T. Steiner, I. Majerz and C. C. Wilson, *Angew. Chem., Int. Ed.*, 2001, **40**, 2651–2654.

50 J. A. Cowan, J. A. K. Howard, G. J. McIntyre, S. M.-F. Lo and I. D. Williams, *Acta Crystallogr., Sect. B: Struct. Sci.*, 2003, **59**, 794–801.

51 A. Parkin, S. M. Harte, A. E. Goeta and C. C. Wilson, *New J. Chem.*, 2004, **28**, 718–721.

52 (*a*) T. Steiner, *Angew. Chem., Int. Ed.*, 2002, **41**, 48–76; (*b*) L. Sobczyk, S. J. Grabowski and T. M. Krygowski, *Chem. Rev.*, 2005, **105**, 3513–3560.

53 R. Kumai, S. Horiuchi, Y. Okimoto and Y. Tokura, *J. Chem. Phys.*, 2006, **125**, 084715.

54 (*a*) M. Sakata, R. Mori, S. Kumazawa, M. Takata and H. Toraya, *J. Appl. Crystallogr.*, 1990, **23**, 526–534; (*b*) M. Sakata and M. Sato, *Acta Crystallogr., Sect. A: Found. Crystallogr.*, 1990, **A46**, 263–270.

55 T. Mitani and T. Inabe, in *Spectroscopy in New Materials*, ed. R. J. H. Clark and R. E. Hester, John Wiley & Sons, Inc., New York, 1993, pp. 291–331.

56 (*a*) T. Mitani, G. Saito and H. Urayama, *Phys. Rev. Lett.*, 1988, **60**, 2299–2302; (*b*) K. Nakasuji, K. Sugiura, T. Kitagawa, J. Toyoda, H. Okamoto, K. Okaniwa, T. Mitani, H. Yamomoto, I. Murata, A. Kawamoto and J. Tanaka, *J. Am. Chem. Soc.*, 1991, **113**, 1862–1864.

57 (*a*) R. Schroeder, L. A. Majewski and M. Grell, *Adv. Mater.*, 2004, **16**, 633–636; (*b*) K. N. N. Unni, R. de Bettignies, S. Dabos-Seignon and J.-M. Nunzi, *Appl. Phys. Lett.*, 2004, **85**, 1823–1825; (*c*) R. C. G. Naber, C. Tanase, P. W. M. Blom, G. H. Gelinck, A. M. Marsman, F. J. Touwslanger, S. Setayesh and D. M. de Leeuw, *Nat. Mater.*, 2005, **4**, 243–248.

58 *Proton Transfer in Hydrogen Bonded Systems*, ed. T. Bountis, Plenum, New York, 1992.